Int. J. Anal. Appl. (2026), 24:205

International Journal of Analysis and Applications

Analyzing the Effects of Lifestyle Modifications on Type 2 Diabetes in India through Atangana-Baleanu Fractional Differential Equations

Masira Khan[1], Amjad Shaikh[2], Sachin Gunjal[3], Kottakkaran Sooppy Nisar[4,*]

[1]*Department of Mathematics and Statistics, Dr. Vishwanath Karad MIT World Peace University, Pune-411038, India*

[2]*Department of Mathematics, AKI's Poona College of Arts, Science and Commerce, Pune, India*

[3]*Department of Mathematics and Statistics, Dr. Vishwanath Karad MIT World Peace University, Pune-411038, India*

[4]*Department of Mathematics, College of Science and Humanities in Al Kharj, Prince Sattam Bin Abdulaziz University, Al Kharj, 11942, Saudi Arabia*

[*]*Corresponding author:* ksnisar1@gmail.com; n.sooppy@psau.edu.sa

Abstract. This study introduces an innovative fractional-order mathematical model aimed at examining the dynamics of type 2 diabetes mellitus through the application of the Atangana-Baleanu-Caputo (ABC) fractional derivative. The proposed model enhances the traditional integer-order diabetes framework by integrating memory and genetic factors, providing a more accurate depiction of disease progression and the impact of lifestyle interventions. The existence and uniqueness of the fractional system are confirmed via the fixed point theorem, thereby affirming its mathematical validity. Approximate analytical solutions are derived through the iterative Laplace transform method (ILTM), while numerical simulations are performed utilizing Mathematica software. Alongside numerical simulations, the analytical properties of the model are confirmed by deriving the basic reproduction number, establishing disease-free equilibrium, and ensuring the positivity of solutions, which guarantees both mathematical consistency and epidemiological feasibility. Simulation results indicate that the fractional order parameter μ significantly affects the temporal dynamics of all compartments-susceptible, afflicted, treated, lifestyle-modified, and prevented. Reduced μ values (enhanced memory effects) postpone illness progression and lifestyle changes, whereas elevated μ values (diminished memory effects) hasten transitions but result in less enduring consequences. The model offers quantitative information regarding the efficacy of lifestyle interventions, allowing policymakers to formulate data-driven plans for diabetes prevention and management. The fractional ABC diabetes model provides a comprehensive and adaptable framework for elucidating the influence of memory on chronic disease dynamics and informing evidence-based public health strategies.

Received: Jan. 23, 2026.

2020 *Mathematics Subject Classification.* 34K37, 35R11, 74S40.

Key words and phrases. Atangana Baleanu Caputo (ABC) operator; fractional diabetes model; existence and uniqueness; stability analysis; numerical simulation; iterative Laplace transform method (ILTM).

https://doi.org/10.28924/2291-8639-24-2026-205
ISSN: 2291-8639

1. Introduction

Diabetes mellitus represents a persistent metabolic condition and an increasingly prevalent silent epidemic that significantly adds to the worldwide challenge of non-communicable diseases. This situation arises when the body is unable to generate adequate insulin or cannot utilize the insulin it produces effectively. Insulin, a hormone produced by the pancreas, plays a crucial role in facilitating the entry of glucose obtained from digested carbohydrates, into body cell, where it is used to produce energy. Under normal physiology, carbohydrates are broken down into glucose, which stimulates the pancreas to release insulin. This insulin enables tissues such as muscle and liver to absorb glucose from the bloodstream. When this mechanism is disrupted, glucose accumulates in the blood, leading to hyperglycemia. This dysfunction not only disturbs carbohydrate metabolism but also adversely affects lipid and protein regulation, underscoring insulin's central role as an anabolic hormone [1].

Diabetes mellitus has emerged as a significant global health challenge in the 21st century. Impacting more than 422 million individuals globally, it regularly appears in the top ten causes of death and disability [18]. Among adults aged 20-79 years, the global prevalence was estimated at 9.3% (463 million) in 2019, which rose to 10.5% (537 million) by 2021. Projections from the international diabetes federation (IDF) indicates a further increase to 12.1% (783 million) by 2045 [32], reflecting the relentless expansion of this chronic condition.

The impact of unmanaged diabetes on health is significant [11]. Individuals with diabetes encounter a significantly elevated risk of macrovascular complications, such as stroke, myocardial infarction, and coronary artery disease, with the likelihood of stroke being estimated at four times greater than that of non-diabetic individuals. Additionally, microvascular complications such as diabetic nephropathy, retinopathy, and neuropathy contribute significantly to long-term morbidity, often resulting in blindness, renal failure, and limb dysfunction. Notably, the prevalence of end-stage kidney disease is tenfold higher among diabetic individuals, and diabetic retinopathy remains a leading cause of preventable adult blindness.

Diabetes mellitus is defined by disrupted insulin metabolism, which can range from total deficiency to varying levels of resistance, leading to the body's failure to efficiently remove glucose from the bloodstream [23]. Three essential physiological factors regulate glucose levels: insulin sensitivity, glucose effectiveness, and pancreatic responsiveness. According to its causes, diabetes mellitus is categorized into three main types [14]:

- Type 1 diabetes mellitus (T1DM) is an autoimmune condition characterized by the destruction of insulin-producing $\beta-$ cells, resulting in minimal or absent insulin production.
- Type 2 diabetes mellitus (T2DM) is the most common form worldwide, marked by insulin resistance and inadequate insulin production.
- Gestational diabetes mellitus (GDM) is a type of diabetes that arises during pregnancy, presenting potential risks to the health of both the mother and the fetus.

The T2DM accounts for nearly 90% of all diabetes cases globally, with approximately 80% of those affected living in low and middle-income countries [35]. India, frequently identified as the diabetes capital of the world, has an estimated 77 million adults diagnosed with diabetes, in addition to nearly 25 million prediabetics who are at a significant risk of progression [22]. Alarmingly, more than 50% of Indians with diabetes remain undiagnosed, leading to delayed treatment and higher complication rates [9, 15]. The prevalence is significantly greater in urban regions, where lifestyle changes characterized by decreased physical activity, dietary modifications, and increasing obesity have intensified the epidemic [28]. The swift urbanization of India, changes in food habits, and sedentary lifestyles have contributed to a significant increase in T2DM. The IDF states that in 2019, India had 77 million individual's with diabetes, a figure anticipated to rise to 134 million by 2045. The ICMR-INDIAB study (2011-2017) indicated urban prevalence rates of $10-14\%$, whereas rural areas exhibited rates of $6-9\%$ [7].

Mathematical modeling is an effective instrument for analyzing dynamic systems and comprehending intricate real-world phenomenon. It enables researchers to convert biological and medical issues into mathematical models, facilitating the analysis of disease transmission, forecasting long-term results, and devising control techniques. Infectious disease modeling has garnered considerable interest in recent decades, especially in light of the persistent worldwide hazards posed by epidemics and pandemics. These models facilitate the prediction of disease dynamics, the assessment of possible outbreaks, and the evaluation of intervention measures, encompassing vaccination, treatment, and quarantine. Omame et al. [25] formulated an integer-order co-infection model for COVID-19 and Dengue, highlighting the need of preventive efforts in Brazil. Models have likewise been employed to investigate co-infections of Zika and Dengue [4], Cholera and Buruli ulcer, as well as syphilis and HPV [16].

Mathematical modeling offers a robust framework for comprehending the intricate dynamics of T2DM, encompassing the regulation of glucose-insulin interactions, $\beta-$ cell functionality, and the enduring effects of lifestyle and treatment interventions. In the biological sciences, mathematical modeling has been essential for many years, providing important insights into several aspects of diabetes mellitus. Notably, the VW model for diabetes was presented by Boutayeb et al. [12] in 2004. The susceptible diabetic complexity UVW model, which was enhanced by Rashid et al. [27], is derived from this VW model. In [19], A. Ferdous built an ODE model to evaluate the effects of lifestyle changes on the T2DM epidemic.

Fractional differential equations (FDEs) models have gained prominence in epidemiology due to their ability to incorporate memory and genetic characteristics that standard integer-order models fail to capture. These characteristics render FDEs especially apt for modeling incubation periods, diminishing immunity, and other prolonged memory effects in disease transmission dynamics [20, 34]. Various fractional operators are employed in epidemiological literature, such as the Caputo, Caputo-Fabrizio, Atangana-Baleanu, and fractal-fractional derivatives, where each operator exhibits distinct kernel characteristics (singular vs non-singular, local vs non-local) that

affect model behavior and numerical analysis [30,31].

The application of fractional calculus to viral infections, including HIV/AIDS, highlights its efficacy, as demonstrated by Shaikh et al. [29]. Yadav et al. [33] formulated a fractional-order model for diabetes mellitus employing the ABC operator. Nisar and Farman [24] examined a fractional-order glucose–insulin monitoring system and analyzed its controllability through proportional-integral-derivative (PID) control. Jeeva et al. [21] utilized the Sumudu transform method in their analysis of a fractional-order T2DM model. Dadhich et al. [13] recently proposed a fractional-order SEIIT (Susceptible–Exposed–Infected–Insulin Treated) model for diabetes. These studies collectively highlight that fractional-order diabetes models effectively represent the hereditary impact of previous states on current glucose-insulin regulation.

1.1. **Mathematical model description.** This study initiates with the formulation of a mathematical model for diabetes mellitus utilizing integer-order derivatives, drawing inspiration from Ferdous [19]. We define the total adult population N(t) at time t as encompassing all individuals aged 20-79 years in India. This population is categorized into five distinct epidemiological compartments: the Susceptible class S(t), the Affected class A(t), the Treated class T(t), the Healthy Lifestyle class H(t), and the Prevented class P(t), such that $N(t) = S(t) + A(t) + T(t) + H(t) + P(t)$. Initially, all adults are regarded as susceptible. A segment of the vulnerable population S engages in health-enhancing practices-like dietary adjustments, consistent exercise, and preventive check-ups—and transitions into the healthy lifestyle category H. The individuals who remain susceptible gradually develop diabetes and transition into the affected class A through various behavioral or physiological risk mechanisms. Individuals in class A who receive clinical intervention move to the treated class T. Furthermore, similar to the biological heredity mechanism examined in previous studies, a minor segment of individuals in the lifestyle-modified class H may still progress to diabetes due to genetic predisposition or lifestyle relapse, reverting back to the affected class A. This model is presented by the following figure 1A.

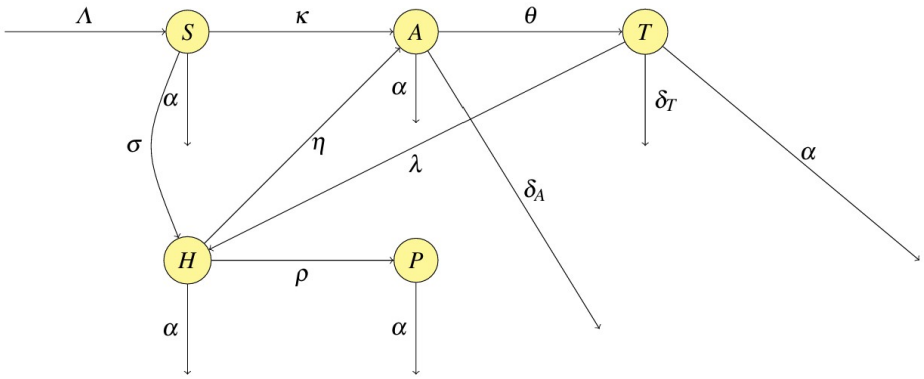

(A)

FIGURE 1. Diagram illustrating the dynamics of T2D in relation to lifestyle interventions.

Integer-order models, although informative on disease dynamics, are constrained in their capacity to incorporate genetic and memory effects, which are essential for understanding the long-term course of chronic diseases like diabetes. To address these restrictions, we enhance Ferdous's model by utilizing the ABC fractional operator [5]. The ABC operator significantly improves the model's capacity to represent real-world complexities. Notwithstanding this constraint, the implementation of the ABC operator signifies a notable methodological progression, reconciling classical integer-order models with the more authentic fractional-order dynamics of diabetes mellitus.
This paper aims to investigate the diabetes model using the framework of fractional order differential equations employing the ABC derivative. Additionally, to investigate the existence and uniqueness of the previously indicated system via fixed point theory. The governing equations of the diabetic model [19] employing the ABC derivative are specified as follows,

$$\begin{cases} {}^{ABC}D_t^{\mu} S(t) = \Lambda - (\alpha + \kappa + \sigma)S(t), \\ {}^{ABC}D_t^{\mu} A(t) = \kappa S(t) - (\theta + \alpha + \delta_A)A(t) + \eta H(t), \\ {}^{ABC}D_t^{\mu} T(t) = \theta A(t) - (\alpha + \delta_T + \lambda)T(t), \\ {}^{ABC}D_t^{\mu} H(t) = \sigma S(t) + \lambda T(t) - (\eta + \alpha + \rho)H(t), \\ {}^{ABC}D_t^{\mu} P(t) = \rho L(t) - \alpha P(t). \end{cases} \tag{1.1}$$

Where ${}^{ABC}D_t^{\mu}$ denotes the AB fractional derivative in Caputo sense for $0 < \mu < 1$, capturing the memory-dependent evolution of each compartment. According to the flow structure depicted in Fig. 1A, the fractional ABD diabetes model is formulated as above system (1.1) of differential equations that includes recruitment Λ, natural mortality α, and diabetes-related mortality from both the affected and treated classes. In this context, σ signifies the rate at which susceptible adults embrace a healthy lifestyle, κ indicates the progression rate from susceptibility to diabetes, η describes the relapse from lifestyle modification to the affected class, and ρ represents the prevention rate from the lifestyle-modified class. The parameter θ represents the treatment rate. Diabetes-related fatalities transpire in categories A and T at frequencies δ_A and δ_T, respectively, under the assumption that $\delta_T < \delta_A$ as individuals who receive treatment demonstrate a reduced likelihood of encountering fatal complications. Individuals who effectively maintain lifestyle enhancements are categorized in the prevented class P, which includes those who achieve stable long-term glycemic control and lower metabolic risk. In this updated model, the new parameter λ signifies the treatment-assisted lifestyle transition, considering individuals in class T who achieve enhanced metabolic outcomes and subsequently shift into the healthy lifestyle class H. This framework effectively captures the dynamics of adult diabetes in India by modeling memory-dependent fractional behavior, highlighting the gradual adoption of lifestyle changes, tendencies for relapse, and the long-term preventive effects that traditional models frequently miss.
The paper is structured as follows. Section 2 presents the definition and a concise overview of the

ABC operator. In Section 3, we introduce an approximation methodology for the ABC fractional diabetes Model via the ILTM. Section 4 is dedicated to demonstrating the existence and uniqueness of solutions for the ABC fractional diabetes model. Section 5 provides a thorough analysis based on the numerical results. Ultimately, Section 6 summarizes the study by emphasizing the principal findings and delineating avenues for future inquiry.

2. Preliminaries and Definitions

Definition 2.1. *[26] The Caputo fractional derivative of a function $\psi(t)$ of order μ, $(n-1<\mu<n)$ is denoted by ${}_a^C D_t^\mu \psi(t)$ and is defined as:*

$$ {}_a^C D_t^\mu \psi(t) = \frac{1}{\Gamma(\mu-n)} \int_a^t \frac{\psi^n(\xi)}{(t-\xi)^{\mu+1-n}} d\xi, \quad (n-1<\mu<n). $$

Definition 2.2. *Following [5], the AB fractional integral of order μ is defined as:*

$$ {}^{AB}I_t^\mu \psi(t) = \frac{1-\mu}{B(\mu)}\psi(t) + \frac{\mu}{B(\mu)\Gamma(\mu)} \int_a^t \psi(\xi)(t-\xi)^\mu d\xi. $$

Definition 2.3. *The ABC fractional derivative is defined as follows [36]:*

$$ {}^{ABC}_0 D_t^\mu \psi(t) = \frac{B(\mu)}{1-\mu} \int_0^t E_\mu \left[-\frac{\mu}{1-\mu}(t-\xi)^\mu \right] \frac{d\psi(\xi)}{d\xi} d\xi. $$

The function $B(\mu)$ acts as a normalization factor, while $E_\mu(z)$ is Mittag–Leffler function.

Definition 2.4. *[6] The Laplace transform for the AB fractional operator of order $0<\mu\leq 1$ is expressed as follows:*

$$ L\left\{ {}^{ABC}_0 D_t^\mu [\psi(t)] \right\}(s) = \frac{B(\mu)}{1-\mu} \frac{s^\mu L\{\psi(t)\}(s) - s^{\mu-1}\psi(0)}{s^\mu + \frac{\mu}{1-\mu}} $$

3. Approximation Technique for the ABC Fractional Diabetes Model

In order to accurately depict the complex transmission dynamics of T2DM, we develop a system (1.1) of fractional differential equations employing the AB derivative in the Caputo sense. This mathematical framework incorporates memory effects and nonlocality, essential for accurately modeling chronic diseases influenced by extended lifestyle patterns and physiological changes. The model categorizes the population into five specific compartments: S(t) representing susceptible individuals, A(t) for newly affected (acute) cases, T(t) for those receiving treatment, H(t) for individuals who have embraced healthy lifestyle changes, and P(t) for those who have recovered or successfully prevented the onset of disease.

The initial conditions in the above system (1.1) are defined as:

$$ S_0(t) = S(0),\ A_0(t) = A(0),\ T_0(t) = T(0),\ H_0(t) = H(0),\ P_0(t) = P(0). $$

The fractional system (1.1) with ABC derivative of order $0<\mu\leq 1$, is written as follows

$$ {}^{ABC}D_t^\mu X_i(t) = \psi_i(t, \mathbf{X}(t)), \qquad \mathbf{X} = (S, A, T, H, P)^\top, \quad i = 1, \ldots, 5 $$

with initial data $S(0), A(0), T(0), H(0), P(0)$. Applying the Laplace transform to each equation and using the Laplace transform of AB derivative rule, we obtain

$$\frac{\frac{B(\mu)}{1-\mu}s^{\mu}\mathcal{L}\{S(t)\} - s^{\mu-1}S(0)}{s^{\mu} + \frac{\mu}{1-\mu}} = \mathcal{L}\{\psi_1(t, \mathbf{X}(t))\},$$

$$\frac{\frac{B(\mu)}{1-\mu}s^{\mu}\mathcal{L}\{A(t)\} - s^{\mu-1}A(0)}{s^{\mu} + \frac{\mu}{1-\mu}} = \mathcal{L}\{\psi_2(t, \mathbf{X}(t))\},$$

$$\frac{\frac{B(\mu)}{1-\mu}s^{\mu}\mathcal{L}\{T(t)\} - s^{\mu-1}T(0)}{s^{\mu} + \frac{\mu}{1-\mu}} = \mathcal{L}\{\psi_3(t, \mathbf{X}(t))\},$$

$$\frac{\frac{B(\mu)}{1-\mu}s^{\mu}\mathcal{L}\{H(t)\} - s^{\mu-1}H(0)}{s^{\mu} + \frac{\mu}{1-\mu}} = \mathcal{L}\{\psi_4(t, \mathbf{X}(t))\},$$

$$\frac{\frac{B(\mu)}{1-\mu}s^{\mu}\mathcal{L}\{P(t)\} - s^{\mu-1}P(0)}{s^{\mu} + \frac{\mu}{1-\mu}} = \mathcal{L}\{\psi_5(t, \mathbf{X}(t))\}.$$

Rearranging, we get

$$\mathcal{L}\{S(t)\} = \frac{S(0)}{s} + \frac{s^{\mu}(1-\mu)+\mu}{s^{\mu}B(\mu)}\mathcal{L}\{\psi_1(t, \mathbf{X}(t))\},$$

$$\mathcal{L}\{A(t)\} = \frac{A(0)}{s} + \frac{s^{\mu}(1-\mu)+\mu}{s^{\mu}B(\mu)}\mathcal{L}\{\psi_2(t, \mathbf{X}(t))\},$$

$$\mathcal{L}\{T(t)\} = \frac{T(0)}{s} + \frac{s^{\mu}(1-\mu)+\mu}{s^{\mu}B(\mu)}\mathcal{L}\{\psi_3(t, \mathbf{X}(t))\},$$

$$\mathcal{L}\{H(t)\} = \frac{H(0)}{s} + \frac{s^{\mu}(1-\mu)+\mu}{s^{\mu}B(\mu)}\mathcal{L}\{\psi_4(t, \mathbf{X}(t))\},$$

$$\mathcal{L}\{P(t)\} = \frac{P(0)}{s} + \frac{s^{\mu}(1-\mu)+\mu}{s^{\mu}B(\mu)}\mathcal{L}\{\psi_5(t, \mathbf{X}(t))\}.$$

Applying the inverse Laplace transform,

$$S(t) = S(0) + \mathcal{L}^{-1}\left[\frac{s^{\mu}(1-\mu)+\mu}{s^{\mu}B(\mu)}\mathcal{L}\{\psi_1(t, \mathbf{X}(t))\}\right],$$

$$A(t) = A(0) + \mathcal{L}^{-1}\left[\frac{s^{\mu}(1-\mu)+\mu}{s^{\mu}B(\mu)}\mathcal{L}\{\psi_2(t, \mathbf{X}(t))\}\right],$$

$$T(t) = T(0) + \mathcal{L}^{-1}\left[\frac{s^{\mu}(1-\mu)+\mu}{s^{\mu}B(\mu)}\mathcal{L}\{\psi_3(t,\mathbf{X}(t))\}\right],$$
$$H(t) = H(0) + \mathcal{L}^{-1}\left[\frac{s^{\mu}(1-\mu)+\mu}{s^{\mu}B(\mu)}\mathcal{L}\{\psi_4(t,\mathbf{X}(t))\}\right],$$
$$P(t) = P(0) + \mathcal{L}^{-1}\left[\frac{s^{\mu}(1-\mu)+\mu}{s^{\mu}B(\mu)}\mathcal{L}\{\psi_5(t,\mathbf{X}(t))\}\right].$$

The solutions obtained through the series method are presented as follows,

$$S = \sum_{n=0}^{\infty} S_n, \quad A = \sum_{n=0}^{\infty} A_n, \quad T = \sum_{n=0}^{\infty} T_n, \quad H = \sum_{n=0}^{\infty} H_n, \quad P = \sum_{n=0}^{\infty} P_n.$$

If a nonlinear bi linear term like $S(t)I(t)$ appears in your model, one may write

$$SI(t) = \sum_{n=0}^{\infty} G_n(t), \qquad G_n(t) = \sum_{j=0}^{n} S_j(t) \sum_{r=0}^{n-1} I_r(t) - \sum_{j=0}^{n-1} S_j(t) \sum_{r=0}^{n-1} I_r(t).$$

By applying the initial conditions, we derive the recursive formula expressed as follows:

$$S_{n+1}(t) = S(0) + \mathcal{L}^{-1}\left[\frac{s^{\mu}(1-\mu)+\mu}{s^{\mu}B(\mu)}\mathcal{L}\{\Lambda - (\alpha+\kappa+\sigma)S_n(t)\}\right],$$

$$A_{n+1}(t) = A(0) + \mathcal{L}^{-1}\left[\frac{s^{\mu}(1-\mu)+\mu}{s^{\mu}B(\mu)}\mathcal{L}\{\kappa S_n(t) - (\theta+\alpha+\delta_A)A_n(t) + \eta H_n(t)\}\right],$$

$$T_{n+1}(t) = T(0) + \mathcal{L}^{-1}\left[\frac{s^{\mu}(1-\mu)+\mu}{s^{\mu}B(\mu)}\mathcal{L}\{\theta A_n(t) - (\alpha+\delta_T+\lambda)T_n(t)\}\right],$$

$$H_{n+1}(t) = H(0) + \mathcal{L}^{-1}\left[\frac{s^{\mu}(1-\mu)+\mu}{s^{\mu}B(\mu)}\mathcal{L}\{\sigma S_n(t) + \lambda T_n(t) - (\eta+\alpha+\rho)H_n(t)\}\right],$$

$$P_{n+1}(t) = P(0) + \mathcal{L}^{-1}\left[\frac{s^{\mu}(1-\mu)+\mu}{s^{\mu}B(\mu)}\mathcal{L}\{\rho H_n(t) - \alpha P_n(t)\}\right].$$

The approximate solution is obtained by taking the limit as $n \to \infty$: $S(t) = \lim_{n\to\infty} S_n(t)$, $A(t) = \lim_{n\to\infty} A_n(t)$, $T(t) = \lim_{n\to\infty} T_n(t)$, $\quad H(t) = \lim_{n\to\infty} H_n(t)$, $P(t) = \lim_{n\to\infty} P_n(t)$.

3.1. **Basic reproduction number ($\mathcal{R}_0$).** The estimated number of secondary diabetes cases caused by a single sick person introduced into a completely susceptible adult population is represented by the basic reproduction number $\mathcal{R}_0$. We use the next-generation matrix approach to calculate $\mathcal{R}_0$.

The infected compartments of the model are the affected and treated classes,

$$x = (A, T).$$

At the disease-free equilibrium (DFE)

$$E_0 = \left(\frac{\Lambda}{\alpha}, 0, 0, 0, 0\right).$$

The infected compartments' Jacobian submatrix is broken down into matrices F (new infections) and V (transition terms), so that

$$\dot{x} = F(x) - V(x).$$

The rates at which new cases of diabetes appear are contained in the matrix F. Since the susceptible population only produces new infections inside the afflicted class, we obtain

$$F = \begin{pmatrix} \kappa S^* & 0 \\ 0 & 0 \end{pmatrix} = \begin{pmatrix} \frac{\kappa\Lambda}{\alpha} & 0 \\ 0 & 0 \end{pmatrix}.$$

Transitions between infected compartments and removals brought on by treatment, mortality, and behavioral changes are described by the matrix V:

$$V = \begin{pmatrix} \theta + \alpha + \delta_A & 0 \\ -\theta & \lambda + \alpha + \delta_T \end{pmatrix}.$$

Let

$$k_1 = \theta + \alpha + \delta_A, \qquad k_2 = \lambda + \alpha + \delta_T.$$

Then,

$$V^{-1} = \begin{pmatrix} \frac{1}{k_1} & 0 \\ \frac{\theta}{k_1 k_2} & \frac{1}{k_2} \end{pmatrix}.$$

The next-generation matrix is given by

$$FV^{-1} = \begin{pmatrix} \frac{\kappa\Lambda}{\alpha k_1} & 0 \\ 0 & 0 \end{pmatrix}.$$

The eigenvalues of FV^{-1} are

$$\lambda_1 = \frac{\kappa\Lambda}{\alpha(\theta + \alpha + \delta_A)}, \qquad \lambda_2 = 0.$$

Hence, the basic reproduction number is given by

$$\mathcal{R}_0 = \frac{\kappa\Lambda}{\alpha(\theta + \alpha + \delta_A)}.$$

While the reproduction number $\mathcal{R}_0$ falls with better treatment initiation θ, lower disease-induced mortality δ_A, and greater natural mortality α, it rises with higher diabetes incidence rate κ and adult recruitment rate Λ. Although it has no direct effect on $\mathcal{R}_0$, the parameter λ, which represents treatment-facilitated behavioral change, is crucial to post-infection dynamics and long-term disease control. Notably, since the matrices F and V are evaluated at equilibrium, the fractional order $\alpha \in (0, 1]$ affects the system's transient dynamics but has no effect on the steady-state value of $\mathcal{R}_0$.

3.2. **Disease-Free Equilibrium (DFE).** We set the model's infected compartments-the affected and treated populations-to zero in order to calculate the disease-free equilibrium (DFE):

$$A(t) = 0, \qquad T(t) = 0.$$

The fractional derivatives disappear at equilibrium, and the steady-state equations fulfill

$$D_t^{\mu} X = 0.$$

For the susceptible class $S(t)$, the equilibrium equation reduces to

$$0 = \Lambda - (\kappa + \alpha)S.$$

Solving for S, we obtain

$$S^* = \frac{\Lambda}{\alpha}.$$

Since there are no infected individuals at the DFE,

$$A^* = 0.$$

Similarly, in the absence of affected individuals,

$$T^* = 0.$$

For the healthy lifestyle class $H(t)$, the equilibrium equation is provided by

$$0 = \sigma S - (\rho + \eta + \alpha)H + \phi T.$$

At the DFE, $T^* = 0$, hence

$$0 = \sigma S^* - (\rho + \eta + \alpha)H^*.$$

Substituting $S^* = \dfrac{\Lambda}{\alpha}$ yields

$$H^* = \frac{\sigma\Lambda}{\alpha(\rho + \eta + \alpha)}.$$

For the prevented class $P(t)$, the equilibrium condition is

$$0 = \rho H - \alpha P.$$

Substituting H^* gives

$$P^* = \frac{\rho\sigma\Lambda}{\alpha^2(\rho + \eta + \alpha)}.$$

Consequently, the ABD diabetic model's disease-free equilibrium is

$$E_0 = \left(\frac{\Lambda}{\alpha},\, 0,\, 0,\, \frac{\sigma\Lambda}{\alpha(\rho + \eta + \alpha)},\, \frac{\rho\sigma\Lambda}{\alpha^2(\rho + \eta + \alpha)}\right).$$

For any positive parameter values, the disease-free equilibrium is biologically possible and exists. It depicts a situation where the population is free of diabetes and people are only found in susceptible, good lifestyle, and prevented compartments.

Lemma 3.1 (Positivity of solutions)**.** *The solutions of the fractional ABD diabetes model are non-negative for all $t \geq 0$, given that the initial conditions are non-negative.*

Proof. We rewrite the fractional ABD diabetes model in the integral form corresponding to the Atangana–Baleanu fractional derivative:

$$X(t) = X(0) + \frac{1-\mu}{\mathcal{B}(\mu)} f(X(t),t) + \frac{\mu}{\mathcal{B}(\mu)\Gamma(\mu)} \int_0^t (t-\xi)^{\mu-1} f(X(\xi),\xi)\, d\xi, \tag{3.1}$$

where

$$X(t) = (S(t), A(t), T(t), H(t), P(t))^T,$$

and $f(X,t)$ denotes the right-hand side of the ABD model. Since $S(0) \geq 0$, suppose for contradiction that there exists a first time $\tau_1 > 0$ such that

$$S(\tau_1) = 0, \qquad S(t) > 0 \text{ for } 0 \leq t < \tau_1,$$

and

$${}^{ABC}D_t^{\mu} S(\tau_1) \leq 0.$$

From the first equation of the model, we have

$${}^{ABC}D_t^{\mu} S(\tau_1) = \Lambda > 0,$$

which contradicts the assumption that ${}^{ABC}D_t^{\mu} S(\tau_1) \leq 0$. Hence, $S(t) \geq 0$ for all $t \geq 0$. Assume similarly that there exists $\tau_2 > 0$ such that

$$A(\tau_2) = 0, \qquad A(t) > 0 \text{ for } 0 \leq t < \tau_2.$$

Evaluating the affected equation at τ_2, we obtain

$${}^{ABC}D_t^{\mu} A(\tau_2) = \kappa S(\tau_2) + \eta H(\tau_2) \geq 0,$$

since all parameters and state variables are non-negative. Thus, $A(t)$ cannot become negative. Suppose there exists $\tau_3 > 0$ such that $T(\tau_3) = 0$ and $T(t) > 0$ for $t < \tau_3$. Then,

$${}^{ABC}D_t^{\mu} T(\tau_3) = \theta A(\tau_3) \geq 0,$$

which prevents $T(t)$ from becoming negative. Assume that $H(t)$ becomes zero for the first time at $\tau_4 > 0$. Then,

$${}^{ABC}D_t^{\mu} H(\tau_4) = \sigma S(\tau_4) + \lambda T(\tau_4) \geq 0,$$

indicating that $H(t)$ is non-negative for all $t \geq 0$. Assume there exists $\tau_5 > 0$ such that $P(\tau_5) = 0$. Assessing the modified equation produces

$${}^{ABC}D_t^{\mu} P(\tau_5) = \rho H(\tau_5) \geq 0,$$

which ensures that $P(t)$ remains non-negative. Therefore, by contradiction and the positivity of recruitment and transition terms, all state variables of the fractional ABD diabetes model remain non-negative for all $t \geq 0$, provided the initial conditions are non-negative. □

4. Existence and Uniqueness of Solutions

Consider the fractional-order model given in (1.1). This equation is rewritten as follows

$$\begin{cases} {}^{ABC}D_t^{\mu} S(t) &= \psi_1(t, S(t)) = \Lambda - (\alpha + \kappa + \sigma)S(t), \\ {}^{ABC}D_t^{\mu} A(t) &= \psi_2(t, A(t)) = \kappa S(t) - (\theta + \alpha + \delta_A)A(t) + \eta H(t), \\ {}^{ABC}D_t^{\mu} T(t) &= \psi_3(t, T(t)) = \theta A(t) - (\alpha + \delta_T + \lambda)T(t), \\ {}^{ABC}D_t^{\mu} H(t) &= \psi_4(t, H(t)) = \sigma S(t) + \lambda T(t) - (\eta + \alpha + \rho)H(t), \\ {}^{ABC}D_t^{\mu} P(t) &= \psi_5(t, P(t)) = \rho H(t) - \alpha P(t). \end{cases} \tag{4.1}$$

Let $S(0) = S_0, \quad A(0) = A_0, \quad T(0) = T_0, \quad H(0) = H_0, \; P(0) = P_0.$
The system (4.1) can be transformed into the Volterra-type integral equation through the application of the ABC fractional integral. The model is articulated as follows:

$$\begin{aligned} S(t) - S(0) &= \frac{1-\mu}{B(\mu)}\{\Lambda - (\alpha + \kappa + \sigma)S(t)\} \\ &\quad + \frac{\mu}{B(\mu)\Gamma(\mu)} \int_0^t \{\Lambda - (\alpha + \kappa + \sigma)S(\xi)\}(t-\xi)^{\mu-1} d\xi, \\ A(t) - A(0) &= \frac{1-\mu}{B(\mu)}\{\kappa S(t) - (\theta + \alpha + \delta_A)A(t) + \eta H(t)\} \\ &\quad + \frac{\mu}{B(\mu)\Gamma(\mu)} \int_0^t \{\kappa S(\xi) - (\theta + \alpha + \delta_A)A(\xi) + \eta H(\xi)\}(t-\xi)^{\mu-1} d\xi, \\ T(t) - T(0) &= \frac{1-\mu}{B(\mu)}\{\theta A(t) - (\alpha + \delta_T + \lambda)T(t)\} \\ &\quad + \frac{\mu}{B(\mu)\Gamma(\mu)} \int_0^t \{\theta A(\xi) - (\alpha + \delta_T)T(\xi)\}(t-\xi)^{\mu-1} d\xi, \\ H(t) - H(0) &= \frac{1-\mu}{B(\mu)}\{\sigma S(t) + \lambda T(t) - (\eta + \alpha + \rho)H(t)\} \\ &\quad + \frac{\mu}{B(\mu)\Gamma(\mu)} \int_0^t \{\sigma S(\xi) - (\eta + \alpha + \rho)H(\xi)\}(t-\xi)^{\mu-1} d\xi, \\ P(t) - P(0) &= \frac{1-\mu}{B(\mu)}\{\rho H(t) - \alpha P(t)\} \\ &\quad + \frac{\mu}{B(\mu)\Gamma(\mu)} \int_0^t \{\rho H(\xi) - \alpha P(\xi)\}(t-\xi)^{\mu-1} d\xi, \end{aligned}$$

where $B(\mu)$ is the normalization function of the ABC derivative and $\Gamma(\cdot)$ is the Gamma function.

Theorem 4.1. *Let $J = [0,T]$ and suppose $S, A, T, H, P \in C(J)$ are bounded on J. Define the kernels (right–hand sides of the model)*

$$\begin{aligned}
\psi_1(t, S(t)) &= \Lambda - (\alpha + \kappa + \sigma)S(t),\\
\psi_2(t, A(t)) &= \kappa S(t) - (\theta + \alpha + \delta_A)A(t) + \eta H(t),\\
\psi_3(t, T(t)) &= \theta A(t) - (\alpha + \delta_T + \lambda)T(t),\\
\psi_4(t, H(t)) &= \sigma S(t) + \lambda T(t) - (\eta + \alpha + \rho)H(t),\\
\psi_5(t, P(t)) &= \rho H(t) - \alpha P(t).
\end{aligned}$$

Then each ψ_i is Lipschitz in its argument with constants $\pi_1 = \alpha + \kappa + \sigma$, $\pi_2 = \theta + \alpha + \delta_A$, $\pi_3 = \alpha + \delta_T + \lambda$, $\pi_4 = \eta + \alpha + \rho$, $\pi_5 = \alpha$. Consequently, if $0 \le \pi_i < 1$, for $i = 1, \dots, 5$, the operators are contractions.

Proof. Let $S_1, S_2 \in C(J)$. Then

$$\begin{aligned}
\|\psi_1(t, S_1(t)) - \psi_1(t, S_2(t))\| &= \| - (\alpha + \kappa + \sigma)(S_1(t) - S_2(t))\|\\
&\le (\alpha + \kappa + \sigma)\|S_1(t) - S_2(t)\| = \pi_1\|S_1(t) - S_2(t)\|.
\end{aligned}$$

For ψ_2, let $A_1, A_2 \in C(J)$ while S, L are fixed (bounded) functions on J:

$$\begin{aligned}
\|\psi_2(t, A_1(t)) - \psi_2(t, A_2(t))\| &= \| - (\theta + \alpha + \delta_A)(A_1(t) - A_2(t))\|\\
&\le (\theta + \alpha + \delta_A)\|A_1(t) - A_2(t)\| = \pi_2\|A_1(t) - A_2(t)\|.
\end{aligned}$$

Similarly,

$$\|\psi_3(t, T_1(t)) - \psi_3(t, T_2(t))\| \le (\alpha + \delta_T + \lambda)\|T_1(t) - T_2(t)\| = \pi_3\|T_1(t) - T_2(t)\|,$$

$$\|\psi_4(t, H_1(t)) - \psi_4(t, H_2(t))\| \le (\eta + \alpha + \rho)\|H_1(t) - H_2(t)\| = \pi_4\|H_1(t) - L_2(t)\|,$$

$$\|\psi_5(t, P_1(t)) - \psi_5(t, P_2(t))\| \le \alpha\|P_1(t) - P_2(t)\| = \pi_5\|P_1(t) - P_2(t)\|.$$

Thus each kernel is Lipschitz in its own variable with constants π_i as stated. If $0 \le \pi_i < 1$, the corresponding operators are contractions.
In light of the model's kernels, the aforementioned equations can be reformulated as

$$S(t) = S(0) + \frac{1-\mu}{B(\mu)}\{\psi_1(t, S(t))\} + \frac{\mu}{B(\mu)\Gamma(\mu)}\int_0^t \{\psi_1(\xi, S(\xi))\}(t-\xi)^{\mu-1}d\xi,$$

$$A(t) = A(0) + \frac{1-\mu}{B(\mu)}\{\psi_2(t, A(t))\} + \frac{\mu}{B(\mu)\Gamma(\mu)}\int_0^t \{\psi_2(\xi, A(\xi))\}(t-\xi)^{\mu-1}d\xi,$$

$$T(t) = T(0) + \frac{1-\mu}{B(\mu)}\{\psi_3(t, T(t))\} + \frac{\mu}{B(\mu)\Gamma(\mu)}\int_0^t \{\psi_3(\xi, T(\xi))\}(t-\xi)^{\mu-1}d\xi,$$

$$H(t) = H(0) + \frac{1-\mu}{B(\mu)}\{\psi_4(t, H(t))\} + \frac{\mu}{B(\mu)\Gamma(\mu)}\int_0^t \{\psi_4(\xi, H(\xi))\}(t-\xi)^{\mu-1}d\xi,$$

$$P(t) = P(0) + \frac{1-\mu}{B(\mu)}\{\psi_5(t, P(t))\} + \frac{\mu}{B(\mu)\Gamma(\mu)}\int_0^t \{\psi_5(\xi, P(\xi))\}(t-\xi)^{\mu-1}d\xi.$$

Therefore, we get the following recursive formula,

$$S_n(t) = S(0) + \frac{1-\mu}{B(\mu)}\{\psi_1(t, S_{n-1}(t))\} + \frac{\mu}{B(\mu)\Gamma(\mu)}\int_0^t \{\psi_1(\xi, S_{n-1}(\xi))\}(t-\xi)^{\mu-1}d\xi,$$

$$A_n(t) = A(0) + \frac{1-\mu}{B(\mu)}\{\psi_2(t, A_{n-1}(t))\} + \frac{\mu}{B(\mu)\Gamma(\mu)}\int_0^t \{\psi_2(\xi, A_{n-1}(\xi))\}(t-\xi)^{\mu-1}d\xi,$$

$$T_n(t) = T(0) + \frac{1-\mu}{B(\mu)}\{\psi_3(t, T_{n-1}(t))\} + \frac{\mu}{B(\mu)\Gamma(\mu)}\int_0^t \{\psi_3(\xi, T_{n-1}(\xi))\}(t-\xi)^{\mu-1}d\xi,$$

$$H_n(t) = H(0) + \frac{1-\mu}{B(\mu)}\{\psi_4(t, H_{n-1}(t))\} + \frac{\mu}{B(\mu)\Gamma(\mu)}\int_0^t \{\psi_4(\xi, H_{n-1}(\xi))\}(t-\xi)^{\mu-1}d\xi,$$

$$P_n(t) = P(0) + \frac{1-\mu}{B(\mu)}\{\psi_5(t, P_{n-1}(t))\} + \frac{\mu}{B(\mu)\Gamma(\mu)}\int_0^t \{\psi_5(\xi, P_{n-1}(\xi))\}(t-\xi)^{\mu-1}d\xi.$$

We will now examine the difference between the iterative terms in the expression.

$$\Theta_{1n}(t) = S_n(t) - S_{n-1}(t) = \frac{1-\mu}{B(\mu)}\Big\{\psi_1\Big(t, S_{n-1}(t)\Big) - \psi_1\Big(t, S_{n-2}(t)\Big)\Big\} + \frac{\mu}{B(\mu)\Gamma(\mu)}\int_0^t \Big\{\psi_1\Big(\xi, S_{n-1}(\xi)\Big) - \psi_1\Big(\xi, S_{n-2}(\xi)\Big)\Big\}(t-\xi)^{\mu-1}d\xi,$$

$$\Theta_{2n}(t) = A_n(t) - A_{n-1}(t) = \frac{1-\mu}{B(\mu)}\Big\{\psi_2\Big(t, A_{n-1}(t)\Big) - \psi_2\Big(t, A_{n-2}(t)\Big)\Big\} + \frac{\mu}{B(\mu)\Gamma(\mu)}\int_0^t \Big\{\psi_2\Big(\xi, A_{n-1}(\xi)\Big) - \psi_2\Big(\xi, A_{n-2}(\xi)\Big)\Big\}(t-\xi)^{\mu-1}d\xi,$$

$$\Theta_{3n}(t) = T_n(t) - T_{n-1}(t) = \frac{1-\mu}{B(\mu)}\Big\{\psi_3\Big(t, T_{n-1}(t)\Big) - \psi_3\Big(t, T_{n-2}(t)\Big)\Big\} + \frac{\mu}{B(\mu)\Gamma(\mu)}\int_0^t \Big\{\psi_3\Big(\xi, T_{n-1}(\xi)\Big) - \psi_3\Big(\xi, T_{n-2}(\xi)\Big)\Big\}(t-\xi)^{\mu-1}d\xi,$$

$$\Theta_{4n}(t) = H_n(t) - H_{n-1}(t) = \frac{1-\mu}{B(\mu)}\Big\{\psi_4\Big(t, H_{n-1}(t)\Big) - \psi_4\Big(t, H_{n-2}(t)\Big)\Big\} + \frac{\mu}{B(\mu)\Gamma(\mu)}\int_0^t \Big\{\psi_4\Big(\xi, H_{n-1}(\xi)\Big) - \psi_4\Big(\xi, H_{n-2}(\xi)\Big)\Big\}(t-\xi)^{\mu-1}d\xi,$$

$$\Theta_{5n}(t) = P_n(t) - P_{n-1}(t) = \frac{1-\mu}{B(\mu)}\Big\{\psi_5\Big(t, P_{n-1}(t)\Big) - \psi_5\Big(t, P_{n-2}(t)\Big)\Big\} + \frac{\mu}{B(\mu)\Gamma(\mu)}\int_0^t \Big\{\psi_5\Big(\xi, P_{n-1}(\xi)\Big) - \psi_5\Big(\xi, P_{n-2}(\xi)\Big)\Big\}(t-\xi)^{\mu-1}d\xi.$$

where $S_n = \sum_{m=0}^{\infty} \Theta_{1m}$, $A_n = \sum_{m=0}^{\infty} \Theta_{2m}$, $T_n = \sum_{m=0}^{\infty} \Theta_{3m}$, $L_n = \sum_{m=0}^{\infty} \Theta_{4m}$, $P_n = \sum_{m=0}^{\infty} \Theta_{5m}$.

Applying the norm of both sides and considering triangular inequality,

$$\begin{aligned}
\|\Theta_{1n}(t)\| &= \|S_n(t) - S_{n-1}(t)\| \\
&\leq \frac{1-\mu}{B(\mu)}\|\psi_1(t, S_{n-1}(t)) - \psi_1(t, S_{n-2}(t))\| \\
&\quad + \frac{\mu}{B(\mu)\Gamma(\mu)} \int_0^t \{\psi_1(\xi, S_{n-1}(\xi)) - \psi_1(\xi, S_{n-2}(\xi))\}(t-\xi)^{\mu-1} d\xi, \\
\|\Theta_{2n}(t)\| &= \|A_n(t) - A_{n-1}(t)\| \\
&\leq \frac{1-\mu}{B(\mu)}\|\psi_2(t, A_{n-1}(t)) - \psi_2(t, A_{n-2}(t))\| \\
&\quad + \frac{\mu}{B(\mu)\Gamma(\mu)} \int_0^t \{\psi_2(\xi, A_{n-1}(\xi)) - \psi_2(\xi, A_{n-2}(\xi))\}(t-\xi)^{\mu-1} d\xi, \\
\|\Theta_{3n}(t)\| &= \|T_n(t) - T_{n-1}(t)\| \\
&\leq \frac{1-\mu}{B(\mu)}\|\psi_3(t, T_{n-1}(t)) - \psi_3(t, T_{n-2}(t))\| \\
&\quad + \frac{\mu}{B(\mu)\Gamma(\mu)} \int_0^t \{\psi_3(\xi, T_{n-1}(\xi)) - \psi_3(\xi, T_{n-2}(\xi))\}(t-\xi)^{\mu-1} d\xi, \\
\|\Theta_{4n}(t)\| &= \|H_n(t) - H_{n-1}(t)\| \\
&\leq \frac{1-\mu}{B(\mu)}\|\psi_4(t, H_{n-1}(t)) - \psi_4(t, H_{n-2}(t))\| \\
&\quad + \frac{\mu}{B(\mu)\Gamma(\mu)} \int_0^t \{\psi_4(\xi, H_{n-1}(\xi)) - \psi_4(\xi, H_{n-2}(\xi))\}(t-\xi)^{\mu-1} d\xi, \\
\|\Theta_{5n}(t)\| &= \|P_n(t) - P_{n-1}(t)\| \\
&\leq \frac{1-\mu}{B(\mu)}\|\psi_5(t, P_{n-1}(t)) - \psi_5(t, P_{n-2}(t))\| \\
&\quad + \frac{\mu}{B(\mu)\Gamma(\mu)} \int_0^t \{\psi_5(\xi, P_{n-1}(\xi)) - \psi_5(\xi, P_{n-2}(\xi))\}(t-\xi)^{\mu-1} d\xi.
\end{aligned}$$

Given that the kernels adhere to the Lipschitz condition, we can derive the following results.

$$\|\Theta_{1n}(t)\| \leq \frac{1-\mu}{B(\mu)}\pi_1\|\Theta_{1(n-1)}(t)\| + \frac{\mu}{B(\mu)\Gamma(\mu)}\pi_1 \int_0^t (t-\xi)^{\mu-1}\|\Theta_{1(n-1)}(\xi)\| d\xi,$$

$$\|\Theta_{2n}(t)\| \leq \frac{1-\mu}{B(\mu)}\pi_2\|\Theta_{2(n-1)}(t)\| + \frac{\mu}{B(\mu)\Gamma(\mu)}\pi_2 \int_0^t (t-\xi)^{\mu-1}\|\Theta_{2(n-1)}(\xi)\| d\xi,$$

$$\|\Theta_{3n}(t)\| \leq \frac{1-\mu}{B(\mu)}\pi_3\|\Theta_{3(n-1)}(t)\| + \frac{\mu}{B(\mu)\Gamma(\mu)}\pi_3\int_0^t (t-\xi)^{\mu-1}\|\Theta_{3(n-1)}(\xi)\|d\xi,$$

$$\|\Theta_{4n}(t)\| \leq \frac{1-\mu}{B(\mu)}\pi_4\|\Theta_{4(n-1)}(t)\| + \frac{\mu}{B(\mu)\Gamma(\mu)}\pi_4\int_0^t (t-\xi)^{\mu-1}\|\Theta_{4(n-1)}(\xi)\|d\xi,$$

$$\|\Theta_{5n}(t)\| \leq \frac{1-\mu}{B(\mu)}\pi_5\|\Theta_{5(n-1)}(t)\| + \frac{\mu}{B(\mu)\Gamma(\mu)}\pi_5\int_0^t (t-\xi)^{\mu-1}\|\Theta_{5(n-1)}(\xi)\|d\xi.$$

This concludes the demonstration of the theorem. □

Theorem 4.2 (Existence of the solution)**.** *The system* (4.1) *with kernels* $\psi_1, \ldots, \psi_5$ *(for* S, A, T, H, P*) has a solution on* $[0,\ t_{\max}]$ *provided there exists* $t_{\max} > 0$ *such that, for each* $j \in \{1,2,3,4,5\}$*,*

$$\frac{\pi_j}{B(\mu)}\left(1-\mu+\frac{t_{\max}^{\mu}}{\Gamma(\mu)}\right) < 1, \qquad 0 < \mu \leq 1,$$

where π_j *are the Lipschitz constants of* ψ_j*.*

Proof. Assume $S(t), A(t), T(t), H(t), P(t)$ are bounded on $[0,\ t_{\max}]$. From the iterative differences $\Theta_{jn}(t) = X_{jn}(t) - X_{j(n-1)}(t)$ ($X_1 = S$, $X_2 = A$, $X_3 = T$, $X_4 = H$, $X_5 = P$) and the inequalities obtained using the Lipschitz property, we get for all $t \in [0,\ t_{\max}]$:

$$\|\Theta_{1n}(t)\| \leq \|S(0)\|\left\{\frac{\pi_1}{B(\mu)}\left(1-\mu+\frac{t_{\max}^{\mu}}{\Gamma(\mu)}\right)\right\}^n,$$

$$\|\Theta_{2n}(t)\| \leq \|A(0)\|\left\{\frac{\pi_2}{B(\mu)}\left(1-\mu+\frac{t_{\max}^{\mu}}{\Gamma(\mu)}\right)\right\}^n,$$

$$\|\Theta_{3n}(t)\| \leq \|T(0)\|\left\{\frac{\pi_3}{B(\mu)}\left(1-\mu+\frac{t_{\max}^{\mu}}{\Gamma(\mu)}\right)\right\}^n,$$

$$\|\Theta_{4n}(t)\| \leq \|H(0)\|\left\{\frac{\pi_4}{B(\mu)}\left(1-\mu+\frac{t_{\max}^{\mu}}{\Gamma(\mu)}\right)\right\}^n,$$

$$\|\Theta_{5n}(t)\| \leq \|P(0)\|\left\{\frac{\pi_5}{B(\mu)}\left(1-\mu+\frac{t_{\max}^{\mu}}{\Gamma(\mu)}\right)\right\}^n.$$

Since each geometric factor is less than 1 by the hypothesis, the series $\sum_{n=0}^{\infty}\Theta_{jn}(t)$ converge uniformly, hence S_n, A_n, T_n, H_n, P_n converge to a solution of the system (4.1) on $[0, t_{\max}]$.

Hence, the functions $\Theta_{1n}(t), \Theta_{2n}(t), \Theta_{3n}(t), \Theta_{4n}(t)$, and $\Theta_{5n}(t)$ exist and are smooth. Moreover, to show that these functions are the solutions of the given system (4.1), we assume that

$$\begin{aligned}
S(t) - S(0) &= S_n(t) - \Delta_{1(n)}(t),\\
A(t) - A(0) &= A_n(t) - \Delta_{2(n)}(t),\\
T(t) - T(0) &= T_n(t) - \Delta_{3(n)}(t),\\
H(t) - H(0) &= H_n(t) - \Delta_{4(n)}(t),\\
P(t) - P(0) &= P_n(t) - \Delta_{5(n)}(t),
\end{aligned} \tag{4.2}$$

where $\Delta_{1(n)}(t), \Delta_{2(n)}(t), \Delta_{3(n)}(t), \Delta_{4(n)}(t)$, and $\Delta_{5(n)}(t)$ represent the remainder terms of the series solution.

Next, we need to demonstrate that these terms converge to zero as we approach infinity, specifically, $\|\Delta_{1(\infty)}(t)\| \to 0,\ \|\Delta_{2(\infty)}(t)\| \to 0,\ \|\Delta_{3(\infty)}(t)\| \to 0,\ \|\Delta_{4(\infty)}(t)\| \to 0,\ \|\Delta_{5(\infty)}(t)\| \to 0.$

Thus, for the term $\Delta_{1(n)}(t)$, we have

$$\begin{aligned}\|\Delta_{1(n)}(t)\| &\leq \frac{1-\mu}{B(\mu)}\|\Phi_1(t,S(t)) - \Phi_1(t,S_{n-1}(t))\| \\ &\quad + \frac{\mu}{B(\mu)\Gamma(\mu)}\int_0^t (t-\xi)^{\mu-1}\|\Phi_1(\xi,S(\xi)) - \Phi_1(\xi,S_{n-1}(\xi))\|d\xi, \\ &\leq \frac{\pi_1}{B(\mu)}\left((1-\mu) + \frac{t_{\max}^{\mu}}{\Gamma(\mu)}\right)\|S(t) - S_{n-1}(t)\|.\end{aligned}$$

Continuing this way recursively, we get

$$\|\Delta_{1(n)}(t)\| \leq B\pi_1^n\left\{\frac{1}{B(\mu)}\left((1-\mu) + \frac{t_{\max}^{\mu}}{\Gamma(\mu)}\right)\right\}^{n+1},$$

where $B = \|S(t) - S_{n-1}(t)\|$.

When we take the limit of both sides as n tends to infinity, we get

$$\|\Delta_{j(\infty)}(t)\| \to 0, \quad j \in \{1,2,3,4,5\}.$$

□

Theorem 4.1 demonstrates that the kernels of the system (4.1) adhere to the Lipschitz condition, which guarantees contraction behavior as long as the constants are maintained below unity. This ensures the stability of the model-minor alterations in population states (such as susceptible or diabetic individuals) result in corresponding shifts, illustrating realistic and gradual dynamics. Theorem 3.2 additionally confirms the existence of at least one solution under specified conditions. The uniform convergence of iterative sequences guarantees the consistency and tractability of the model. From a biological perspective, this indicates that the system (4.1) progresses along a distinct and foreseeable path throughout all compartments-susceptible, affected, treated, lifestyle-modified, and prevented-when initiated with realistic data.

5. Numerical Simulations and Discussions

5.1. **Numerical Approximations.** In this section, we analyze the numerical simulations of the ABD diabetes model (1.1) using the real-population formulation, in which each state variable represents the absolute number of individuals rather than normalized proportions. Accordingly, the total adult population at time t is expressed as $N(t) = S(t) + A(t) + T(t) + L(t) + P(t)$, where S(t) denotes the susceptible adults (non-diabetics at risk), A(t) represents undiagnosed diabetics (newly affected), T(t) denotes diagnosed individuals receiving medical treatment, H(t) refers to individuals who have adopted lifestyle modifications, and P(t) corresponds to those who have

successfully prevented or recovered from diabetes through sustained lifestyle adaptation.

Based on the most recent International Diabetes Federation (IDF) country statistics, the base year for the simulations is 2024, with the adult population of India estimated at $N(0) = 947,373,600$ and $89,826,900$ adults living with diabetes. With 43% of diabetes cases remaining undiagnosed the initial values for the model compartments are computed as $S(0) = 857,546,700$, $A(0) = 38,625,567$, $T(0) = 51,201,333$, $H(0) = 0$, $P(0) = 0$.

Given that the average life expectancy in India is 72 years, the demographic rate α is computed as $\alpha = \frac{1}{72} = 0.0139$. The birth (recruitment) rate is calculated as $\Lambda = \alpha N(0) = 0.0139 \times 94,73,73600 = 13,157,967$ persons per year. Since 10.5% of Indian adults have diabetes, according to the IDF, the diabetes incidence rate from the vulnerable class is set at $\kappa = 0.13$. In addition, 43% of diabetes cases in India are reportedly still undetected. As a result, 57% is the treatment rate, and the parameter θ is set as $\theta = 0.57$. According to recent national estimates, 4% of all cases of diabetes result in mortality from complications associated to the disease. In light of this data, $\delta_A = 0.04$ for affected individuals and $\delta_T = 0.015$ for treated individuals in that order. The remaining parameters-representing lifestyle adoption, behavioral relapse, and prevention success-are assumed based on prior modeling studies and expert judgment, $\sigma = 0.06$ (rate of lifestyle adoption), $\rho = 0.12$ (rate of successful prevention), $\eta = 0.03$ (rate of relapse from lifestyle class). These baseline values are summarized in Table 1 and are used consistently across all simulations involving the ABC fractional diabetes model. The fractional order μ is varied across simulations to assess the impact of memory effects on disease progression and the effectiveness of lifestyle interventions.

Description of Parameter and Variable		**Value**	**Reference**
Rate of adult population entry (birth/recruitment)	Λ	13,157,967	Estimated
Natural adult mortality rate	α	0.0139	[17]
Rate of becoming affected from susceptible class	κ	0.565	[10]
Rate of receiving treatment	θ	0.35	[10]
Rate of adopting healthy lifestyle	σ	0.06	Assumed
Rate of transitioning to prevented class	ρ	0.12	Assumed
Rate of treatment-facilitated lifestyle transition	λ	0.15	Assumed
Rate of relapse from lifestyle to affected class	η	0.03	Assumed
Death rate from complications in affected class	δ_A	0.04	[10]
Complication-related death rate in treated class	δ_T	0.015	[10]

TABLE 1. Values of the parameters used to simulate the diabetic model (1.1)

t	Susceptible Population S(t)			
	$\mu = 0.45$	$\mu = 0.65$	$\mu = 0.85$	$\mu = 1$
1	7.17127×10^8	7.37076×10^8	7.67237×10^8	7.91109×10^8
2	5.74165×10^8	5.72948×10^8	5.88491×10^8	6.06381×10^8
3	4.46327×10^8	4.05944×10^8	3.70152×10^8	3.43749×10^8
4	3.28522×10^8	2.50552×10^8	1.52873×10^8	5.93239×10^7
5	2.03731×10^8	1.00218×10^8	-3.96001×10^7	-1.91870×10^8

TABLE 2. Numerical result of susceptible population S(t) for fractional parameter μ

t	Affected Population A(t)			
	$\mu = 0.45$	$\mu = 0.65$	$\mu = 0.85$	$\mu = 1$
1	9.78681×10^7	9.8233×10^7	8.99448×10^7	7.93518×10^7
2	5.79451×10^7	1.02587×10^8	1.45291×10^7	1.64792×10^8
3	-1.40297×10^8	-5.1461×10^7	8.52821×10^7	1.84729×10^8
4	-5.40355×10^8	-4.63264×10^8	-2.43991×10^8	-4.45319×10^7
5	-1.18007×10^9	-1.23434×10^9	-1.02964×10^9	-7.80162×10^8

TABLE 3. Numerical result of Affected population A(t) for fractional parameter μ

t	Treated Population T(t)			
	$\mu = 0.45$	$\mu = 0.65$	$\mu = 0.85$	$\mu = 1$
1	8.39934×10^7	7.57247×10^7	6.553×10^7	5.9431×10^7
2	1.23663×10^8	1.32583×10^8	1.20685×10^7	1.03565×10^8
3	5.74757×10^7	1.51115×10^8	2.12497×10^8	2.16968×10^8
4	-2.92018×10^8	-5.18276×10^7	2.33325×10^8	3.72006×10^8
5	-1.16235×10^9	-8.01425×10^8	-1.17777×10^8	3.55186×10^8

TABLE 4. Numerical result of Treated population T(t) for fractional parameter μ

t	Healthy Lifestyle Population H(t)			
	$\mu = 0.45$	$\mu = 0.65$	$\mu = 0.85$	$\mu = 1$
1	5.8374×10^7	5.09917×10^7	3.88505×10^7	2.88376×10^7
2	1.0575×10^8	1.12104×10^8	1.11321×10^8	1.06603×10^8
3	1.23259×10^8	1.52891×10^8	1.85278×10^8	2.07056×10^8
4	9.89114×10^7	1.47307×10^8	2.22309×10^8	2.86460×10^8
5	2.27721×10^7	6.97177×10^7	1.76697×10^8	2.83587×10^8

TABLE 5. Numerical result of Healthy Lifestyle Population H(t) for fractional parameter μ

t	Prevented Population P(t)			
	$\mu = 0.45$	$\mu = 0.65$	$\mu = 0.85$	$\mu = 1$
1	3.6690×10^6	2.22199×10^6	898846	292612
2	1.6200×10^7	1.29382×10^7	7.94669×10^6	4.53527×10^6
3	3.59937×10^7	3.52491×10^7	2.85874×10^7	2.17235×10^7
4	5.79801×10^7	6.75416×10^7	6.83448×10^7	6.31865×10^7
5	7.41594×10^7	1.02231×10^8	1.26589×10^8	1.37093×10^8

TABLE 6. Numerical result of Prevented population P(t) for fractional parameter μ

The simulation results across Tables 2 to 6 reveal how fractional dynamics influence the evolution of each compartment over time. As the fractional order μ increases from 0.45 to 1.0, the system transitions from memory-influenced behavior to classical dynamics. Lower μ values (stronger memory effects) lead to slower transitions but sharper peaks in affected and treated populations. In contrast, higher μ values result in faster lifestyle adoption and prevention, with larger healthy and prevented populations by year 5. Overall, the model highlights that fractional dynamics capture delayed behavioral responses, making them valuable for simulating long-term public health strategies.

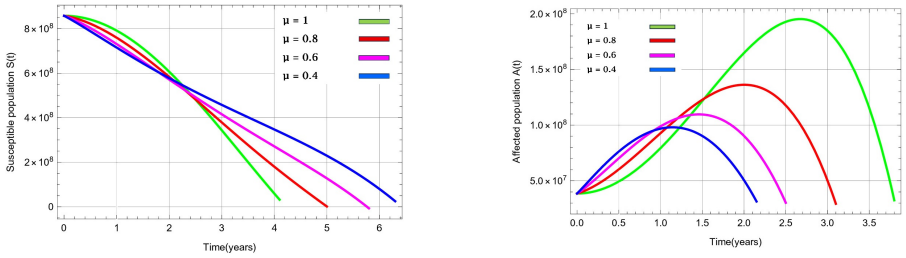

(A) (B)

FIGURE 2. Dynamical behavior of a) Susceptible population S(t) and b) Affected population A(t) for various values of μ with respect to time(days)

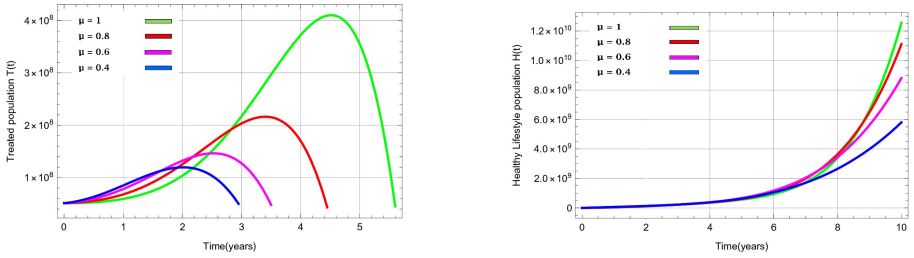

(A) (B)

FIGURE 3. Dynamical behavior of a) Treated population T(t) and b) Healthy Lifestyle population H(t) for various values of μ with respect to time(days)

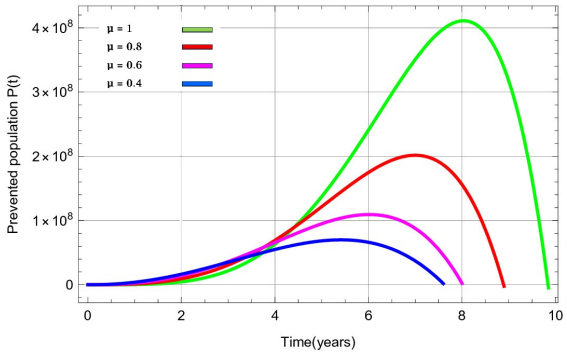

FIGURE 4. Dynamical behavior of Prevented population P(t) for various values of μ with respect to time(days)

Figures 2A to 4 depict the compartmental dynamics of the fractional-order ABD diabetes model, employing the ABC derivative and ILTM for fractional orders $\mu \in \{0.4, 0.6, 0.8, 1.0\}$. These simulations demonstrate the influence of memory effects on disease progression and the outcomes of interventions. Figure 2A shows that S(t) declines more rapidly for higher fractional orders. When $\mu = 1$, the susceptible population collapses quickly, while lower values of μ (e.g., 0.4) substantially delay this decline. This demonstrates that stronger memory effects slow the rate at which individuals leave the susceptible class, thereby reducing the effective transmission speed. The trajectories never rise again after the initial drop, indicating a persistent reduction of the susceptible population. Figure 2B depicts the dynamics of the affected class A(t), showing an initial rise followed by a peak whose magnitude and timing depend strongly on the fractional order. For the classical case $\mu = 1$, the affected population reaches the largest and latest peak, indicating rapid accumulation of undiagnosed cases. As μ decreases, the peaks occur earlier and with substantially lower amplitude, demonstrating the moderating influence of memory effects on disease progression. For $\mu = 0.4$, the peak is both smallest and earliest, reflecting strong memory-driven damping in the transition from susceptibility to the affected class. Figure 3A shows the temporal evolution of the treated population T(t) over a 6-year simulation period. For all fractional orders, the treated class initially increases as affected individuals enter medical care, followed by a peak and subsequent decline. The magnitude and timing of the peak are highly sensitive to the fractional order. For the classical case $\mu = 1$, treatment numbers rise sharply and reach the largest peak around the fifth year. As μ decreases, both the height and duration of the growth phase reduce: peaks occur earlier at approximately 3.3, 2.7, and 2.2 years for $\mu = 0.8, 0.6$, and 0.4, respectively, with substantially lower maximum values. Figure 3B shows that the lifestyle-modified population H(t) grows continuously throughout the 10-year period for all values of μ. Higher fractional orders $\mu = 1$ and 0.8 produce faster growth, reflecting quicker adoption of healthy behaviors, while lower values $\mu = 0.6$ and 0.4 result in slower long-term accumulation. The divergence among the curves becomes more pronounced after year 6, indicating that memory effects primarily influence the long-term spread of lifestyle modification. Overall, increasing μ accelerates behavioral transition,

whereas stronger memory reduces the pace of lifestyle adoption.

Figure 4 shows that the prevented population P(t) increases steadily during the initial years and reaches its peak between years $6-9$, depending on the fractional order μ. Higher values of $\mu(\mu = 1$ and $0.8)$ lead to substantially larger prevention gains, with sharper and earlier peaks, indicating more effective transition into the prevention class. In contrast, lower orders $(\mu = 0.6$ and $0.4)$ produce smaller and delayed peaks, reflecting slower accumulation of individuals achieving successful prevention. Overall, reduced memory effects (higher μ) enhance prevention outcomes, whereas stronger memory $(\mu = 0.4)$ slows the progress of long-term diabetes prevention. The sensitive population S(t) declines continuously as people join impacted or lifestyle-modified groups. Treatment and prevention reduce class A(t). The treated population T(t) initially rises, peaking at year 4, due to medical intervention, then declines. The healthy lifestyle class H(t) increases significantly, peaking around year 5, showing effective behavioral adoption. Meanwhile, the prevented class P(t) continues to expand, proving that lifestyle interventions effectively improve T2DM resistance. Overall, simulations show that fractional order μ considerably impacts compartment dynamics. As μ rises from 0.4 to 1.0, the system changes faster and the afflicted population decreases faster. The behavior highlights the significance of fractional modeling in memory-dependent processes and implies that the ABC derivative is a reliable framework for chronic disease simulation.

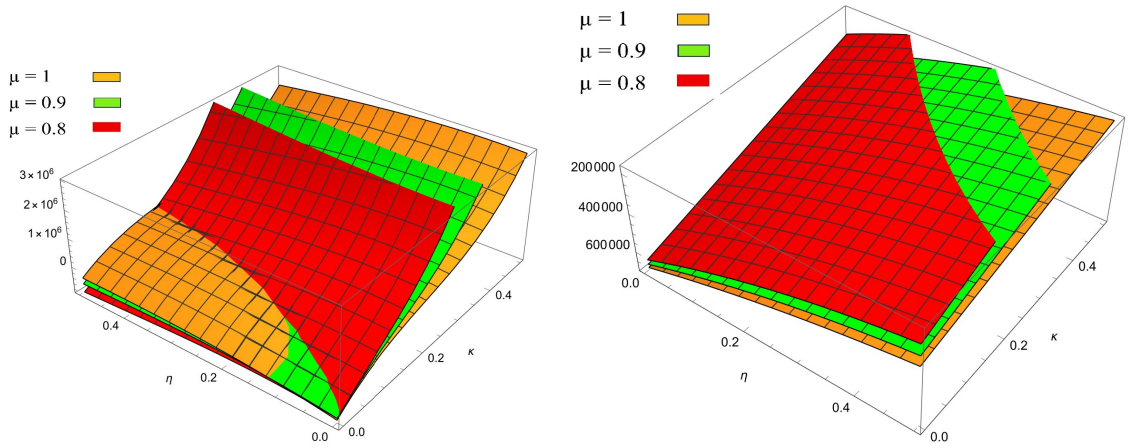

(A) (B)

FIGURE 5. Influence of the transition rates κ (from the susceptible group) and η (from the lifestyle-modified group) on the dynamics of (a) the affected population A(t) and (b) the prevented population P(t) for various values of μ.

Figures 5A and 5B examine the impact of transition rates from the susceptible κ and lifestyle-modified η compartments on the dynamics of T2DM, particularly under fractional orders. Values of μ are 1.0, 0.9, and 0.8. The illustration in Figure 5A presents Affected Population A(t) reflects the number of affected individuals rises with increasing κ and η, most sharply under $\mu = 1.0$ (orange surface), indicating minimal memory resistance. The influence of κ is significantly greater

than that of η, highlighting the necessity to mitigate early transitions from susceptibility in order to lessen disease burden. Figure 5B demonstrating Prevented Population class P(t) shows that with increasing values of κ and η, there is a decline in the prevented population for all μ values. The most significant decline is observed at $\mu = 1.0$, whereas enhanced memory effects at $\mu = 0.8$ contribute to the maintenance of prevention outcomes. This highlights the essential importance of early intervention in the vulnerable population to maintain long-term resistance to diabetes.

5.2. **Population predictions by compartment.** The compartmental predictions of the fractional diabetes model for India offer a comprehensive overview of the evolution of each population group over the next decade, influenced by varying fractional orders μ. The susceptible population S(t) shows a steady decrease over the simulation period from 2024 to 2034, with more pronounced declines observed at elevated μ levels. For $\mu = 1$, the susceptible pool is anticipated to decline sharply after 2026, with projections indicating a reduction of over $40 - 45\%$ by 2030, illustrating an increased transition into affected, treated, and lifestyle-modified groups. Conversely, with a value of $\mu = 0.4$, the decline unfolds at a more gradual pace, resulting in a significantly larger susceptible population by 2034. The population under consideration A(t) experiences a significant increase in the initial years of the simulation. For $\mu \geq 0.8$, the affected class peaks around $2026 - 2027$, followed by a noticeable decline as treatment and lifestyle interventions start to take precedence in the flow. With reduced memory orders $(\mu = 0.4 - 0.6)$, the peak is anticipated to occur sooner, approximately in 2025, and at a significantly lower magnitude. However, the decline is more gradual, indicating a sustained period of moderate disease prevalence and an extended burden of disease. The treated class T(t) exhibits a consistent upward trajectory across all fractional orders. For $\mu = 1$, there is a notable acceleration in treatment uptake post 2026, culminating in the treated population peaking around $2029 - 2030$. For fractional orders below 0.8, the increase initiates earlier but reaches its peak sooner and at lower levels-typically stabilizing between $2026 - 2028$ suggesting diminished treatment access or a slower transition into formal care. The lifestyle-modified class H(t) demonstrates consistent growth throughout the entire ten-year period. When $\mu = 1$, the adoption of lifestyle changes progresses swiftly after 2027, achieving significantly elevated levels by $2032 - 2034$, indicating a robust reaction to behavioral interventions. With lower μ, growth experiences a slower and more delayed trajectory, with significant expansion becoming evident only post 2030. This suggests that memory effects impede the pace of behavioral shifts towards healthier lifestyle practices. The population that successfully avoids diabetes through sustained lifestyle modification, denoted as P(t), shows significant growth for $\mu = 1$, with the most substantial increases occurring between 2028 and 2033, ultimately reaching its peak by 2034. With reduced μ, growth continues at a moderate pace, and prevention levels stay significantly below the classical case, even by the conclusion of the simulation. This suggests that significant memory effects postpone the overall influence of preventive measures.

The projections indicate that higher fractional orders ($\mu = 1$) result in more rapid transitions, quicker peaks, and earlier stabilization across all compartments. In contrast, lower orders lead to a

more prolonged progression, diminishing peak intensity while extending the duration of disease persistence. The findings highlight the significance of memory-dependent fractional dynamics in influencing long-term diabetes trends within the Indian population.

5.3. **Model importance in lifestyle intervention impact assessment.** The fractional-order diabetes model emphasizes the significant influence of the fractional order $\mu-$ indicative of population memory-on the efficacy of lifestyle interventions throughout India. Increased values of μ (indicating weaker memory) result in more rapid behavioral transitions, enhanced lifestyle adoption, and earlier achievements in prevention. Conversely, reduced μ values (indicating stronger memory) hinder these processes, leading to an extended disease burden and a delay in the effectiveness of interventions. The ABC fractional framework effectively integrates memory-driven dynamics, allowing it to capture the gradual behavioral responses, long-term adherence patterns, and delayed shifts that are frequently seen in chronic disease management-elements that traditional integer-order models typically miss. The model measures the impact of different levels of lifestyle intervention effectiveness on the progression of each compartment-susceptible, affected, treated, lifestyle-modified, and prevented-offering valuable insights for the design of targeted programs. Simulations tailored with demographic and epidemiological data specific to India indicate that enhancing awareness, implementing structured treatment pathways, and promoting community-level lifestyle programs can significantly alleviate the national diabetes burden and expedite prevention outcomes. The fractional-order model functions as an effective data-driven instrument for predicting the effects of interventions, shaping public health strategies, and assessing long-term diabetes prevention policies focused on lifestyle changes within the Indian population.

5.4. **The fractional ABD diabetes model suggested preventive measures.** The fractional ABD diabetes model for India highlights that long-term, memory-aware public health strategies are essential for reducing the rising burden of T2DM. Because fractional dynamics show that behavioral change occurs gradually and accumulates over several years, short-term initiatives alone are insufficient. Instead, sustained, community-centered programs—such as group exercise initiatives, subsidized yoga and fitness sessions, and school-based nutrition training-are shown to progressively expand the lifestyle-modified and prevented populations in the model simulations. These findings emphasize the need for multi-year health promotion efforts that reinforce behavioral consistency. To maintain adherence and reduce relapse, the model underscores the importance of monitoring and reinforcement mechanisms. Digital health applications that track diet, daily activity, and treatment adherence can provide timely alerts and motivational feedback, thereby lowering the relapse parameter η and strengthening the treatment-induced lifestyle transition parameter λ. In addition, early detection remains critical. Regular screening through mobile diagnostic vans, annual diabetes camps, and workplace health drives across urban and semi-urban regions can improve timely diagnosis and reduce the affected burden by boosting the treatment-transition parameter θ.

The parameter sensitivities of the model (σ, ρ, λ, and η) show that enhancing community awareness, improving accessibility of structured lifestyle programs, and strengthening treatment adherence pathways have substantial impact on downstream prevention. Policy-based tools—such as nutritional labeling, sugar taxation, incentives for gym membership, or subsidized sports facilities—can accelerate lifestyle adoption (σ) and prevention success (ρ). Fractional-order simulations allow policymakers to predict the long-term benefits of such interventions before implementation, supporting evidence-driven planning. Community peer-support networks and local cultural programs further help sustain behavioral change, especially in populations with strong memory effects (low μ). Incentives such as insurance premium discounts, preventive health vouchers, or tax benefits can enhance participation in wellness initiatives and strengthen long-term prevention. These strategies align with national efforts such as the NPCDCS, Ayushman Bharat, Fit India Movement, and state-level diabetes awareness campaigns. Together, the fractional model results provide a robust scientific foundation for designing long-duration, population-wide diabetes prevention programs tailored to India's demographic structure, behavioral patterns, and healthcare priorities.

6. Conclusion

This study formulated and examined a fractional-order diabetes model utilizing the ABC derivative, building upon Ferdous's integer-order approach to incorporate memory-driven dynamics in the progression of T2DM. The establishment of existence and uniqueness for the fractional model was achieved through the application of the fixed point theorem, thereby guaranteeing both mathematical consistency and biological validity. The incorporation of the basic reproduction number, disease-free equilibrium, and positivity analysis enhances the theoretical framework of the fractional ABD diabetes model, affirming its well-posedness and appropriateness for long-term population-level diabetes forecasting. The ILTM was utilized to approximate the solutions of the nonlinear fractional system, with Mathematica software facilitating efficient numerical simulations and visualization of the compartmental dynamics.

The results demonstrate that the fractional order μ plays a pivotal role in determining the temporal evolution of each compartment. Lower μ values, representing stronger memory effects, delay the onset, peak, and stabilization of disease states, indicating a slower yet more persistent disease trajectory. Conversely, higher μ values, corresponding to weaker memory effects, accelerate transitions but may lead to less sustained behavioral or epidemiological outcomes. These insights highlight that populations with stronger memory effects may require prolonged and consistent intervention programs, whereas populations with weaker memory respond more quickly to lifestyle and treatment initiatives.

From a public health perspective, the ability to tune μ provides a powerful framework for simulating diverse epidemiological scenarios and optimizing lifestyle intervention strategies, healthcare resource allocation, and prevention policies. Overall, the fractional ABD diabetes model not only

advances the mathematical understanding of chronic disease dynamics but also offers a practical decision-support tool for designing targeted, long-term diabetes management programs. Future extensions may include stochastic modeling, parameter sensitivity analysis, and data-driven calibration to enhance predictive accuracy and policy relevance.

Acknowledgement: The authors extend their appreciation to Prince Sattam bin Abdulaziz University for funding this research work through the project number (PSAU/2025/01/34222).

Conflicts of Interest: The authors declare that there are no conflicts of interest regarding the publication of this paper.

References

[1] World Health Organization, Diabetes, https://www.who.int/news-room/fact-sheets/detail/diabetes, Accessed December 31, 2024.

[2] International Diabetes Federation, IDF Diabetes Atlas 10th Edition 2021, International Diabetes Federation, (2021). https://idf.org/about-diabetes/resources/idf-diabetes-atlas-2021.

[3] HealthCentral, https://www.healthcentral.com.

[4] A.I. Adekunle, O.A. Adegboye, E. Gayawan, E.S. McBryde, Is Nigeria Really on Top of COVID-19? Message from Effective Reproduction Number, Epidemiol. Infect. 148 (2020), e166. https://doi.org/10.1017/S0950268820001740.

[5] A. Atangana, D. Baleanu, New Fractional Derivatives with Nonlocal and Non-Singular Kernel: Theory and Application to Heat Transfer Model, Therm. Sci. 20 (2016), 763–769. https://doi.org/10.2298/TSCI160111018A.

[6] A. Atangana, I. Koca, Chaos in a Simple Nonlinear System with Atangana–Baleanu Derivatives with Fractional Order, Chaos Solitons Fractals 89 (2016), 447–454. https://doi.org/10.1016/j.chaos.2016.02.012.

[7] R.M. Anjana, M. Deepa, R. Pradeepa, The Icmr-Indiab Study: Results from the National Study on Diabetes in India, J. Indian Inst. Sci. 103 (2023), 21–32. https://doi.org/10.1007/s41745-023-00359-8.

[8] Freedom from Diabetes, Freedom from Diabetes Research Foundation, https://www.freedomfromdiabetes.org/research.

[9] M. Bramhankar, M. Dhar, Diseases Burden and Epidemiological Transition Status at the National and Sub-National Level in India: A Contemporary Perspective, Discov. Public Health 22 (2025), 63. https://doi.org/10.1186/s12982-025-00453-5.

[10] Diabetic Association of India, Pune Branch, http://daipune.com/English/index.html.

[11] E. Cousin, M.I. Schmidt, K.L. Ong, R. Lozano, A. Afshin, et al., Burden of Diabetes and Hyperglycaemia in Adults in the Americas, 1990–2019: A Systematic Analysis for the Global Burden of Disease Study 2019, Lancet Diabetes Endocrinol. 10 (2022), 655–667. https://doi.org/10.1016/S2213-8587(22)00186-3.

[12] A. Boutayeb, E. Twizell, K. Achouayb, A. Chetouani, A Mathematical Model for the Burden of Diabetes and Its Complications, Biomed. Eng. Online 3 (2004), 20. https://doi.org/10.1186/1475-925X-3-20.

[13] S. Dadhich, M.P. Yadav, Kritika, A Fractional-Order Differential Equation Model of Diabetes Mellitus Type SEIIT, Int. J. Math. Ind. 16 (2024), 2450001. https://doi.org/10.1142/S2661335224500011.

[14] C. DeClue, M. Gonzalez, A.B. Bradley, B.G. Carranza-Leon, G. Srivastava, The Latest Trends in the Management of Type 1 and Type 2 Diabetes Mellitus, Endocrines 5 (2024), 566–584. https://doi.org/10.3390/endocrines5040041.

[15] D.A. Reddy, M. E., Epidemiological Transition in India and Determinants That Are Shifting Disease Burden: A Systematic Review, Univers. J. Public Health 12 (2024), 781–791. https://doi.org/10.13189/ujph.2024.120418.

[16] A. Omame, D. Okuonghae, U.E. Nwafor, B.U. Odionyenma, A Co-Infection Model for HPV and Syphilis with Optimal Control and Cost-Effectiveness Analysis, Int. J. Biomath. 14 (2021), 2150050. https://doi.org/10.1142/S1793524521500509.

[17] Our World in Data, Life Expectancy, https://ourworldindata.org/grapher/life-expectancy.
[18] D. Glovaci, W. Fan, N.D. Wong, Epidemiology of Diabetes Mellitus and Cardiovascular Disease, Curr. Cardiol. Rep. 21 (2019), 21. https://doi.org/10.1007/s11886-019-1107-y.
[19] A. Ferdous, An Ordinary Differential Equation Model for Assessing the Impact of Lifestyle Intervention on Type 2 Diabetes Epidemic, Healthc. Anal. 4 (2023), 100271. https://doi.org/10.1016/j.health.2023.100271.
[20] S. Jahan, S. Ahmed, P. Yadav, K.S. Nisar, Fibonacci Wavelet Method for the Numerical Solution of a Fractional Relaxation–Oscillation Model, Partial. Differ. Equ. Appl. Math. 8 (2023), 100568. https://doi.org/10.1016/j.padiff.2023.100568.
[21] N. Jeeva, K.M. Dharmalingam, P.U. Preetha, D. Sreepal, A Fractional Order Study of the Type 2 Diabetes Model Using the Sumudu Transform Method, Indian J. Nat. Sci. 15 (2024), 83193–83201.
[22] V. Kumar, History of Diabetes in India, in: RSSDI Textbook of Diabetes Mellitus, Jaypee Brothers Medical Publishers, (2023).
[23] A. Makroglou, J. Li, Y. Kuang, Mathematical Models and Software Tools for the Glucose-Insulin Regulatory System and Diabetes: An Overview, Appl. Numer. Math. 56 (2006), 559–573. https://doi.org/10.1016/j.apnum.2005.04.023.
[24] K.S. Nisar, M. Farman, Investigation of Fractional Order Model for Glucose-Insulin Monitoring with PID and Controllability, Sci. Rep. 15 (2025), 8128. https://doi.org/10.1038/s41598-025-91231-5.
[25] A.U. Rehman, R. Singh, P. Agarwal, Modeling, Analysis and Prediction of New Variants of COVID-19 and Dengue Co-Infection on Complex Network, Chaos, Solitons Fractals 150 (2021), 111008. https://doi.org/10.1016/j.chaos.2021.111008.
[26] I. Podlubny, Fractional Differential Equations, Academic Press, 1999.
[27] S. Rashid, F. Jarad, T.M. Jawa, A Study of Behaviour for Fractional Order Diabetes Model via the Nonsingular Kernel, AIMS Math. 7 (2022), 5072–5092. https://doi.org/10.3934/math.2022282.
[28] A. Ramachandran, C. Snehalatha, S. Mary, B. Mukesh, A.D. Bhaskar, et al., The Indian Diabetes Prevention Programme Shows That Lifestyle Modification and Metformin Prevent Type 2 Diabetes in Asian Indian Subjects with Impaired Glucose Tolerance (IDPP-1), Diabetologia 49 (2006), 289–297. https://doi.org/10.1007/s00125-005-0097-z.
[29] A. Shaikh, K.S. Nisar, V. Jadhav, S.K. Elagan, M. Zakarya, Dynamical Behaviour of HIV/AIDS Model Using Fractional Derivative with Mittag-Leffler Kernel, Alex. Eng. J. 61 (2022), 2601–2610. https://doi.org/10.1016/j.aej.2021.08.030.
[30] A. Shaikh, A. Tassaddiq, K.S. Nisar, D. Baleanu, Analysis of Differential Equations Involving Caputo–Fabrizio Fractional Operator and Its Applications to Reaction–Diffusion Equations, Adv. Differ. Equ. 2019 (2019), 178. https://doi.org/10.1186/s13662-019-2115-3.
[31] A. Shaikh, S. Howal, K.S. Nisar, Malaria and Malnutrition Dynamics in Children Using the Caputo–Fabrizio Fractional Derivative, Eur. J. Pure Appl. Math. 18 (2025), 6981. https://doi.org/10.29020/nybg.ejpam.v18i4.6981.
[32] H. Sun, P. Saeedi, S. Karuranga, M. Pinkepank, K. Ogurtsova, et al., IDF Diabetes Atlas: Global, Regional and Country-Level Diabetes Prevalence Estimates for 2021 and Projections for 2045, Diabetes Res. Clin. Pract. 183 (2022), 109119. https://doi.org/10.1016/j.diabres.2021.109119.
[33] P. Yadav, S. Jahan, K. Shah, O.J. Peter, T. Abdeljawad, Fractional-Order Modelling and Analysis of Diabetes Mellitus: Utilizing the Atangana-Baleanu Caputo (ABC) Operator, Alex. Eng. J. 81 (2023), 200–209. https://doi.org/10.1016/j.aej.2023.09.006.
[34] P. Yadav, S. Jahan, K.S. Nisar, Fractional Order Mathematical Model of Ebola Virus Under Atangana–Baleanu–Caputo Operator, Results Control. Optim. 13 (2023), 100332. https://doi.org/10.1016/j.rico.2023.100332.
[35] Y. Zheng, S.H. Ley, F.B. Hu, Global Aetiology and Epidemiology of Type 2 Diabetes Mellitus and Its Complications, Nat. Rev. Endocrinol. 14 (2017), 88–98. https://doi.org/10.1038/nrendo.2017.151.

[36] O. J. Peter, A. S. Shaikh, M. O. Ibrahim, K. Sooppy Nisar, D. Baleanu, et al., Analysis and Dynamics of Fractional Order Mathematical Model of COVID-19 in Nigeria Using Atangana-Baleanu Operator, Comput. Mater. Contin. 66 (2021), 1823–1848. https://doi.org/10.32604/cmc.2020.012314.